doi:10.1016/j.jmb.2010.06.010 J. Mol. Biol. (2010) 400, 1067–1077

JMB

Available online at www.sciencedirect.com

ScienceDirect

ELSEVIER

Multiple Unfolding Events during Native Folding of the *Tetrahymena* Group I Ribozyme

Yaqi Wan[1]†, Hyejean Suh[2]†, Rick Russell[1]* and Daniel Herschlag[2]*

[1]*Department of Chemistry and Biochemistry, Institute for Cellular and Molecular Biology, University of Texas at Austin, Austin, TX 78712, USA*

[2]*Department of Biochemistry, Stanford University, Stanford, CA 94305-5307, USA*

Received 27 January 2010; received in revised form 16 April 2010; accepted 4 June 2010
Available online 10 June 2010

Edited by J. Doudna

Despite the ubiquitous nature of misfolded intermediates in RNA folding, little is known about their physical properties or the folding transitions that allow them to continue folding productively. Folding of the *Tetrahymena* group I ribozyme includes sequential accumulation of two intermediates, termed I_{trap} and misfolded (M). Here, we probe the structure and folding transition of I_{trap} and compare them to those of M. Hydroxyl radical and dimethyl sulfate footprinting show that both I_{trap} and M are extensively structured and crudely resemble the native RNA. However, regions of the core P3–P8 domain are more exposed to solvent in I_{trap} than in M. I_{trap} rearranges to continue folding nearly 1000-fold faster than M, and urea accelerates folding of I_{trap} much less than M. Thus, the rate-limiting transition from I_{trap} requires a smaller increase in exposed surface. Mutations that disrupt peripheral tertiary contacts give large and nearly uniform increases in re-folding of M, whereas the same mutations give at most modest increases in folding from I_{trap}. Intriguingly, mutations within the peripheral element P5abc give 5- to 10-fold accelerations in escape from I_{trap}, whereas ablation of P13, which lies on the opposite surface in the native structure, near the P3–P8 domain, has no effect. Thus, the unfolding required from I_{trap} appears to be local, whereas the unfolding of M appears to be global. Further, the modest effects from several mutations suggest that there are multiple pathways for escape from I_{trap} and that escape is aided by loosening nearby native structural constraints, presumably to facilitate local movements of nucleotides or segments that have not formed native contacts. Overall, these and prior results suggest a model in which the global architecture and peripheral interactions of the RNA are achieved relatively early in folding. Multiple folding and re-folding events occur on the predominant pathway to the native state, with increasing native core interactions and cooperativity as folding progresses.

Keywords: *Tetrahymena* ribozyme; group I intron; catalytic RNA; RNA folding; hydroxyl radical footprinting

Introduction

A hallmark of RNA folding *in vitro* is the presence and accumulation of misfolded intermediates, referred to as 'kinetic traps', which must partially unfold to continue folding productively to the native state.[1–3] Far less is known about RNA folding *in vivo*, but multi-step folding and assembly processes are common, and these processes are assisted by RNA binding proteins and chaperones.[3–6] To understand why and how RNA assembly and folding pathways have evolved and how they function, it is necessary to unravel the intrinsic folding properties of RNAs.

Nearly every RNA whose folding has been studied has been found to be rate-limited for folding by the presence of one or more trapped intermediates, typically diagnosed by an increased folding rate in the presence of a denaturant such as urea.[7–11] However, relatively little is known about the physical properties of these misfolded states and the folding transitions that lead to their formation and decay.

**Corresponding authors.* E-mail addresses: rick_russell@mail.utexas.edu; herschla@stanford.edu.

† Y.W. and H.S. contributed equally to this work.

Abbreviation used: DMS, dimethyl sulfate.

The *Tetrahymena* group I ribozyme has provided a powerful system for studies of RNA folding for more than a decade. Early folding studies demonstrated the presence of intermediates,[12–14] one of which was shown to be kinetically trapped and stabilized by native structure within the peripheral element P5abc.[9] Subsequent delineation of a kinetic framework established that there are two distinct intermediates that are formed sequentially, termed I_{trap} and M (Scheme 1).[15] It was not clear whether one or a mixture of these was probed in the early experiments. However, the kinetic framework delineated conditions that give selective accumulation of each species to a large fraction of the total population.[10,15]

We used this framework to characterize the long-lived intermediate M.[10,16] Probes of global and local structure indicated that the structure of M is highly similar to that of the native state, N, with differences localized to the conserved core, yet activity assays demonstrated that re-folding of M to the native state is very slow and involves extensive disruption of structure. These and other results led to a structural model in which the misfolded species is a local topological isomer of the native state that requires extensive unfolding to convert to the native state.[10]

Here, we explore the earlier folding intermediate, I_{trap}, and compare its structural features and folding properties with those of the later intermediate M, as determined previously[10] or as measured side by side herein. We find that I_{trap} and M are both extensively structured and appear to share structural features, but elements of the conserved core are more exposed to solvent in I_{trap}. Further, the folding properties of these two intermediates are dramatically different from each other, as I_{trap} refolds to N much more readily and with much less extensive structural disruption. These differences

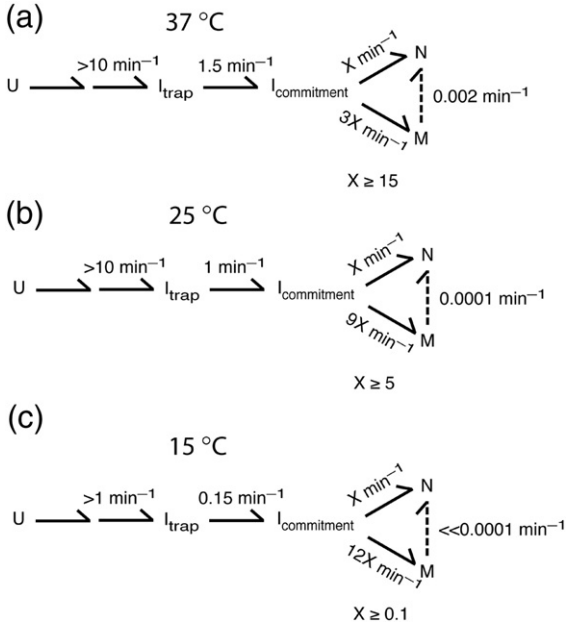

Scheme 1. Rate constants for folding and misfolding of the Tetrahymena ribozyme at different temperatures.

may reflect the challenges associated with formation of cooperative networks of interactions as the RNA proceeds to its active conformation.

Results and Discussion

The secondary structure and tertiary arrangement of the *Tetrahymena* ribozyme are shown in Fig. 1. The native structure of the RNA is stabilized by five long-range, peripheral contacts, indicated by double-headed arrows. The peripheral elements that form these contacts are conserved in the C1 subclass of group I introns, and they surround the universally conserved catalytic core.[17–19] In the previously studied misfolded intermediate M, each of the peripheral contacts is formed, and the core is protected from solution-based hydroxyl radicals with a pattern that is nearly identical with that for the native ribozyme. Indeed, the M state can carry out a catalytic reaction using one of the two normal ribozyme substrates.[10] Nevertheless, conversion to the native state is extraordinarily slow and is enhanced by 10- to 200-fold upon disruption of any of the long-range tertiary contacts.[10] These and additional data led us to propose that the native peripheral contacts trap a topological isomer of the native ribozyme that prevents proper binding of one of the substrates and requires global unfolding to allow rearrangement to the native state, despite the high level of similarity of the two structures.

Here, we probe the properties and behavior of a kinetic trap that is earlier on the folding pathway, referred to as I_{trap} (Scheme 1). I_{trap} is formed by essentially the entire ribozyme population when folding is initiated by adding divalent cation (Mg^{2+}) to a solution of ribozyme in low or moderate concentrations of monovalent cations,[20,21] and we have used these conditions to populate and study I_{trap}.

Chemical footprinting of I_{trap}

To probe the tertiary structure of the I_{trap} folding intermediate, we performed hydroxyl radical footprinting using Fe(II)–ethylene dinitrilotetraacetic acid.[22] We also used dimethyl sulfate (DMS) footprinting as a probe of the base-pairing faces of adenosine and cytidine nucleotides.[23–26] After forming I_{trap} by incubating the ribozyme briefly with Mg^{2+} ion,[10,11,15] we performed footprinting for a time that is sufficiently short to prevent the ribozyme from progressing significantly to the more stable native and misfolded structures (see Materials and Methods). To allow direct comparisons between I_{trap} and other species, we footprinted the native, misfolded, and unfolded ribozyme (U) species side by side.

Changes in solvent exposure in I_{trap} relative to the unfolded ribozyme were readily apparent by hydroxyl radical footprinting (Fig. 2a). Similar to both the native and misfolded structures, I_{trap} is protected within the core of the ribozyme (P4, P6,

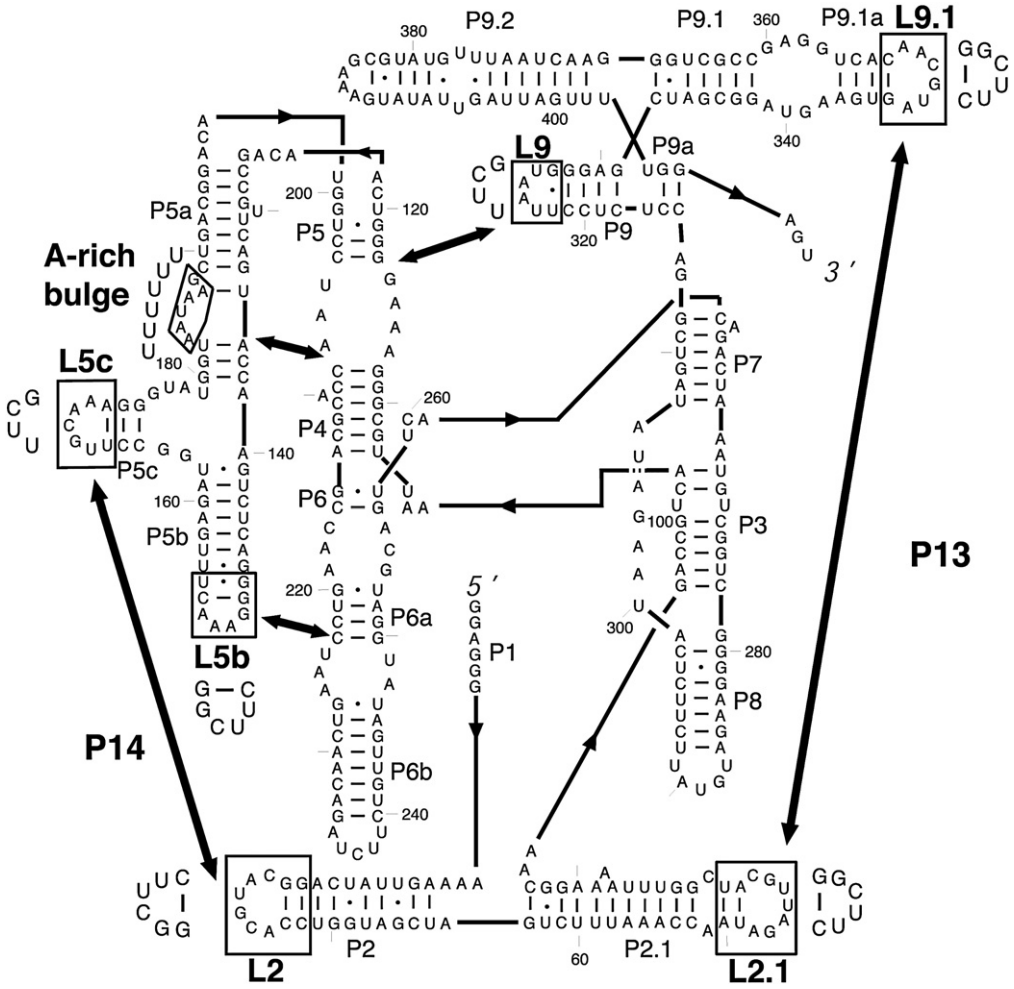

Fig. 1. Secondary structure of the *Tetrahymena* group I ribozyme. The five long-range contacts are indicated by thick arrows, and the mutations made to abolish these tertiary contacts are indicated with boxes, with the substituted residues shown adjacent to each box.

and P6a), as well as in peripheral elements that pack against the core (P5abc and P9.1a), and it is enhanced in exposure in several of the same regions as the native and misfolded structures (L2.1, P5a, L6b, and P9.1). The corresponding patterns of structure formation, relative to unfolded ribozyme, are shown for M in Fig. 2b and for N in Fig. S1a. Thus, many of the structural features of the I_{trap} intermediate appear to be similar to the native and misfolded species.

DMS footprinting also revealed substantial protection in I_{trap}, relative to U, and gave similar patterns for I_{trap} and both the native and misfolded species (Fig. 2a and c and Fig. S1b). This similarity suggests that interconversion between these species involves at most local changes in secondary structure. DMS footprinting also provided evidence for formation in I_{trap} of at least some of the peripheral tertiary contacts. Protections were observed in loops L5b (A151–A153), L5c (C170–A172), and the A-rich

Fig. 2. Hydroxyl radical and DMS footprinting of the I_{trap} folding intermediate. (a–c) Comparisons of footprinting pattern for different intermediates displayed on the secondary structure. Shaded boxes beneath the nucleotide letters represent results of hydroxyl radical footprinting, and boxes next to the letters represent results of DMS footprinting.[10] The color of each box corresponds to the difference in band intensity and, therefore, the difference in exposure to the chemical probe of the indicated nucleotide between the two ribozyme species in the comparison (see Materials and Methods for details). (a) Comparison of I_{trap} with the unfolded ribozyme. Nucleotides that are protected in I_{trap}, that is, modified by the probe to a lesser extent, are blue, and those that are exposed in I_{trap} are yellow. (b) Comparison of M and U. Nucleotides that are protected in M are blue and those that are more exposed in M are yellow. (c) Direct comparison of M and I_{trap}. Nucleotides that are protected in M relative to I_{trap} are blue, and those that are exposed in M are yellow. In (a)–(c), the nucleotides with the most prominent changes in DMS reactivity are highlighted with asterisks (see Materials and Methods). (d and e) Comparisons of hydroxyl radical footprinting of the native ribozyme with I_{trap} (d) or M (e), with results displayed on the model of the native tertiary structure. Only the most prominent changes are displayed, with regions that are protected in the native state shown in cyan and those that are enhanced shown in yellow (see Materials and Methods).

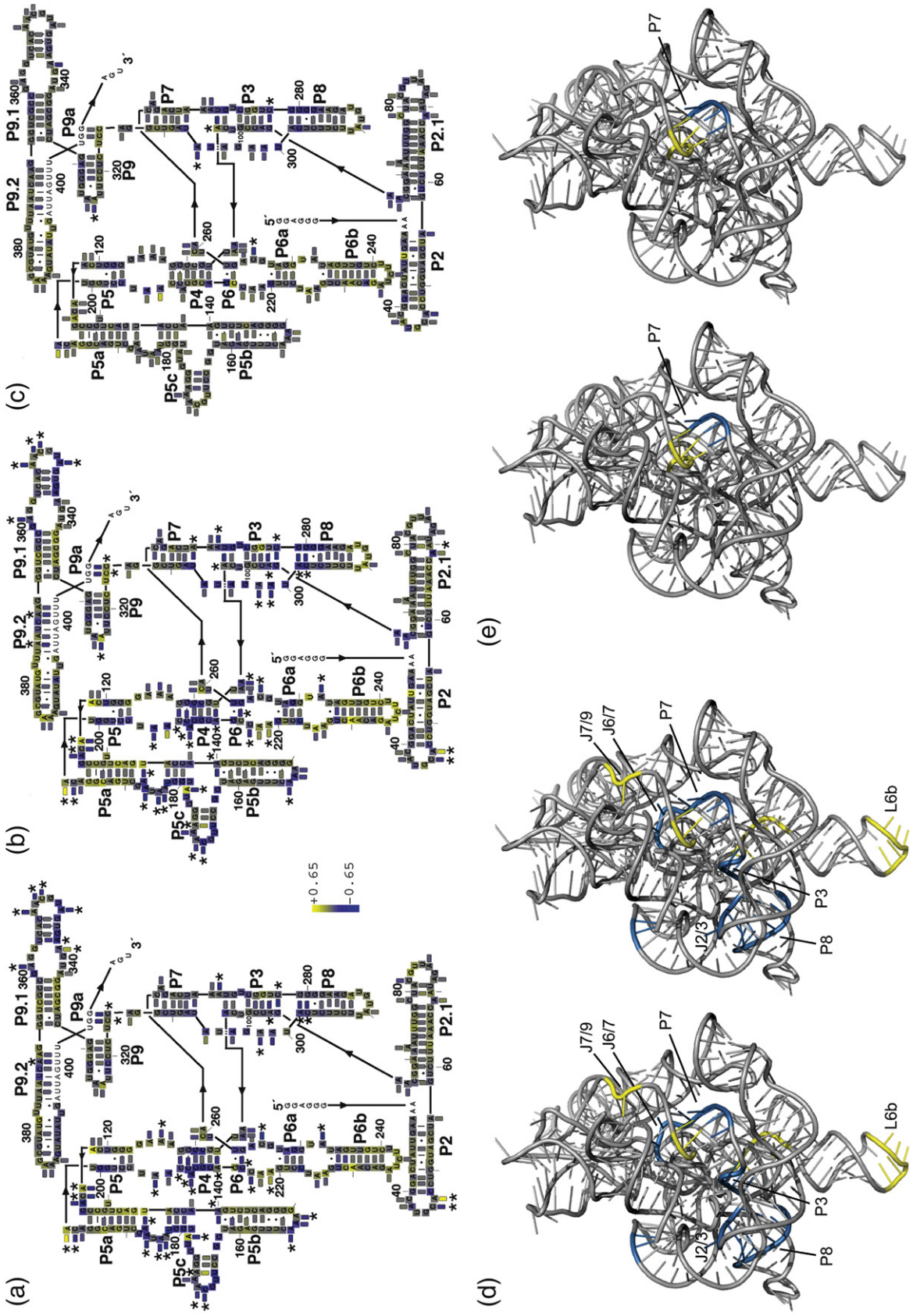

Fig. 2 *(legend on previous page)*

bulge (A183, A184, and A186), suggesting that the three tertiary contacts involving P5abc are formed (see Fig. 1). Protection was also observed in L9.1 (A347, C350–A352), which pairs with L2.1 to form P13. Additionally, the DMS pattern of L2.1 was similar to that of the native state,[10] with modest protection at A74 and C79 and enhanced modification adjacent to the loop (A69) relative to U. Together, these observations suggest that P13 is formed in I_{trap}.

In summary, chemical footprinting provides evidence for extensive structure formation in I_{trap}, including formation of four of the five long-range tertiary contacts. Support for the fifth contact (L9/P5) and independent support for three of the contacts (P14, L5b/J6a, and P5a/P4) comes from the mutagenesis experiments described in the next section.

Despite the extensive similarities, significant differences also exist between the footprinting patterns of I_{trap} and the other folded structures (N and M). Pronounced differences in protection from hydroxyl radicals between the native and misfolded species were reported within P7 of the core,[10] and these differences were largely reproduced under the conditions used here (A263–A270 and U307–G312, Fig. S1c)‡. In this region, I_{trap} is indistinguishable from M, and both intermediates show large differences relative to N (Fig. 2c–e and Fig. S1b and c). Thus, during the transition from I_{trap} to N, the 5′-strand of P7 becomes protected from solvent, whereas in the transition from I_{trap} to M, it remains exposed. Similarly, in the localized regions that give pronounced differences between N and M in reactivity to DMS (A218–A219 in J6/6a and A342 in J9.1/9.1a), I_{trap} gives levels of exposure that are similar to M. There are also significant differences in I_{trap} relative to M that were visible in hydroxyl radical footprinting (Fig. 2c–e). The most prominent differences are within the core, in J7/3, J3/8, J2/3, and J8/7, where each segment is more exposed in I_{trap}. There are also smaller changes in accessibility scattered throughout the structure. Thus, there is apparently a reorganization that is centered on the core during the folding transition from I_{trap}. Consistent with this model, these regions were shown in time-resolved footprinting experiments to be protected on the time scale that would be expected for further folding from I_{trap}.[27] DMS footprinting revealed additional significant differences in modification of a small number of nucleotides (Fig. 2c and Fig. S1b). Nucleotide C255, near the interface of the P4–P6 and P3–P8 domains, was protected in M and N relative to I_{trap}, raising the possibility of a rearrangement at or near the domain interface. Nucleotides C278 and A103, within P3, and A306, within J8/7, were also protected from DMS modification in M and N relative to I_{trap}, providing further support for a rearrangement in the P3–P8 domain of the core.

In summary, the observed changes in solvent exposure of core elements suggest that there is substantial reorganization of the core subsequent to I_{trap} formation. The high degree of similarity of the DMS footprinting patterns of I_{trap}, M, and N suggests that there are no large differences in secondary structure. Indeed, even the 'unfolded' state ('U' in Scheme 1) is thought to include most of the secondary-structure elements present in the final native RNA structure§.[21]

Escape from I_{trap}: Faster and with less structural disruption than for the later kinetic trap, M

It was shown previously that both I_{trap} and M give folding transitions to N (i.e., a fraction of I_{trap} folds to N without first forming M; see Scheme 1), but the properties of these folding transitions differ substantially.[15,20,29] M is much longer-lived than I_{trap}, with a rate constant for further folding of 0.002 min^{-1} at 37 °C and 10 mM Mg^{2+} compared to 1.5 min^{-1} for further folding of I_{trap}.[15,20] In addition, folding of M to N slows sharply with increasing Mg^{2+} (5–100 mM), whereas folding from I_{trap} to N is insensitive to Mg^{2+} concentration across this range.[15] Here, we further probe the properties of the folding transition from I_{trap} by determining the effects of adding urea and eliminating tertiary contacts by mutation, and we compare these effects with those on the folding transition from M.

The rate constant for formation of N from I_{trap} was determined by monitoring cleavage of the oligonucleotide substrate $CCCUCUA_5$ (S) upon initiation of tertiary folding by Mg^{2+} addition. Because substrate cleavage is much faster than overall folding, detection of the cleavage product provides a probe for the rate of overall folding, which is limited in rate by the transition from I_{trap} to N (for the fraction of the ribozyme that avoids M).[20,30] The addition of urea gave a modest increase in the rate constant for N formation from I_{trap} (Fig. 3). The increase corresponds to an m value of 0.56 kcal mol^{-1} M^{-1}, equivalent to the equilibrium m value

‡ Consistent with previous work, nucleotides 263–270 showed protection in the native state relative to the misfolded state. On the other strand of P7 (nucleotides 307–312), the patterns differed substantially between N and M, again consistent with the earlier work.[10] However, a small enhancement observed previously in the N state became more prominent (U307-G309), and the adjacent protection became less prominent (U310-G312), such that only the enhancement is large enough to be shown in Fig. 2e (yellow). It is not clear whether the difference between this work and the earlier work is caused by the changes in solution conditions or by unknown differences in the experiment or analysis, but this difference in the results does not affect the conclusions.

§ There are limited changes in secondary structure between the unfolded and native conformations, most notably the formation of the long-range P3 pseudoknot in N, which replaces a local pairing interaction termed alt P3.[21,28] The correct P3 pairing also appears to be present in the M state,[10] but it is not yet clear whether P3 or alt P3 is formed in I_{trap}.

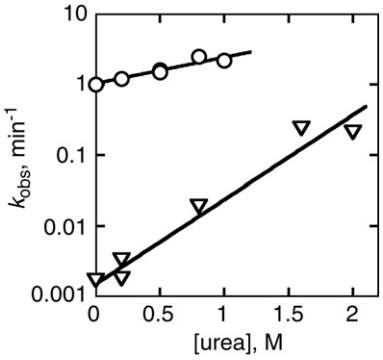

Fig. 3. Acceleration by urea of I_{trap} folding to the native state (○). Data for re-folding of M under the same conditions (37 °C, 10 mM Mg^{2+}) are included for comparison (▽, data from Ref. 10). Across the range of urea concentrations shown for measurements of I_{trap} folding, the rate constant was much larger than that for re-folding of M, allowing a robust determination of the rate constant for the transition from I_{trap} to the native state. At higher urea concentrations (1–2 M), these rate constants become more similar to each other, as shown by the convergence of the lines, such that only the re-folding of M can be measured accurately.

for the disruption of 5–6 base pairs.[31] In contrast, folding from M to N is much more strongly dependent on urea concentration, with an *m* value of 1.7 kcal mol^{-1} M^{-1}, equivalent to disruption of 23 base pairs.[10,31]

Protection of the core elements was monitored previously using binding of complementary oligonucleotides followed by RNase H cleavage, and this transition gave a rate constant of 1 min^{-1} and an *m* value of 0.45 kcal mol^{-1} M^{-1}.[9,12] Based on the conditions used and the similar folding rates and *m* value, this earlier work most likely followed the escape from I_{trap}. Protection of the core from hydroxyl radicals was previously observed to give rate constants in the same range and a modest urea dependence,[27,32,33] suggesting that the transition from I_{trap} was followed in this earlier work as well, although alternative pathways appeared to be populated significantly at the higher temperature of 42 °C in these studies.[27,32,33]

As a further probe of the degree and nature of unfolding in the escape from I_{trap}, we examined the effects of disrupting peripheral tertiary contacts by mutation (see Fig. 1), using activity as a folding monitor as above. Previous work showed that contact disruption can affect the intermediates populated early in folding, at least with higher concentrations of Na^+ ion.[34] Nevertheless, the dominant folding pathways for all of the mutants appear to include formation of the late folding intermediates I_{trap} and M,[10,34] allowing us to probe the properties of these intermediates in folding of the mutated ribozymes.

Disruption of tertiary contacts generally increased the rate of folding from I_{trap}, suggesting that partial unfolding of the periphery facilitates the transition (Fig. 4 and Table S1). This observation is consistent with previous results indicating that structure within P5abc stabilizes a misfolded intermediate, presumably I_{trap} as noted above.[9] On the other hand, the mutational effects on I_{trap} folding were modest, with no contact disruptions giving larger than a 5- to 10-fold effect. For comparison, re-folding of each ribozyme mutant from the M state was measured under the same conditions (Fig. 4). The magnitudes of the increases in re-folding rate from M were somewhat larger than observed previously at higher temperature and lower Mg^{2+} concentration[10] and were much larger than for re-folding of I_{trap} (100- to 1000-fold for M *versus* <10-fold for I_{trap}). The mutagenesis results are consistent with the effects of urea, described above, suggesting that substantially greater unfolding is required for continued folding of M than I_{trap}.

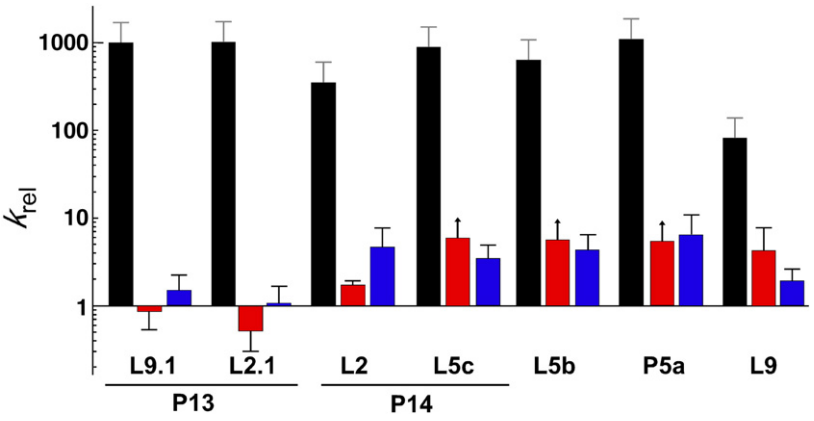

Fig. 4. Effects of tertiary contact disruptions on re-folding of I_{trap} and M. Re-folding to the native state from I_{trap} and M. Black bars, re-folding of M to the native state (25 °C, 50 mM Mg^{2+}). Red bars, re-folding of I_{trap} to the native state under the same conditions. Blue bars, re-folding of I_{trap} under conditions that slow folding and therefore allow detection of the larger effects (11 °C, 50 mM Mg^{2+}). Data are shown relative to the corresponding values for the wild-type ribozyme, which were measured in side-by-side reactions. These values are as follows: 2×10^{-5} min^{-1} for re-folding of M, 1.5±0.4 min^{-1} for re-folding of I_{trap} at 25 °C, and 0.30±0.14 min^{-1} for re-folding of I_{trap} at 11 °C. Measurements for folding from I_{trap} were performed at least three times and are shown with error bars corresponding to the standard deviation from these measurements. For some ribozyme variants, only a lower limit for the folding rate constant from I_{trap} was determined at 25 °C, as indicated by upward-pointing arrows above the red bars. For re-folding from M, measurements were performed once, giving relative values that were qualitatively similar to previous measurements performed at 37 °C and 10 mM Mg^{2+}.[10] The gray error bars show the expected uncertainties based on previous measurements of re-folding, approximately 1.5- to 2-fold.

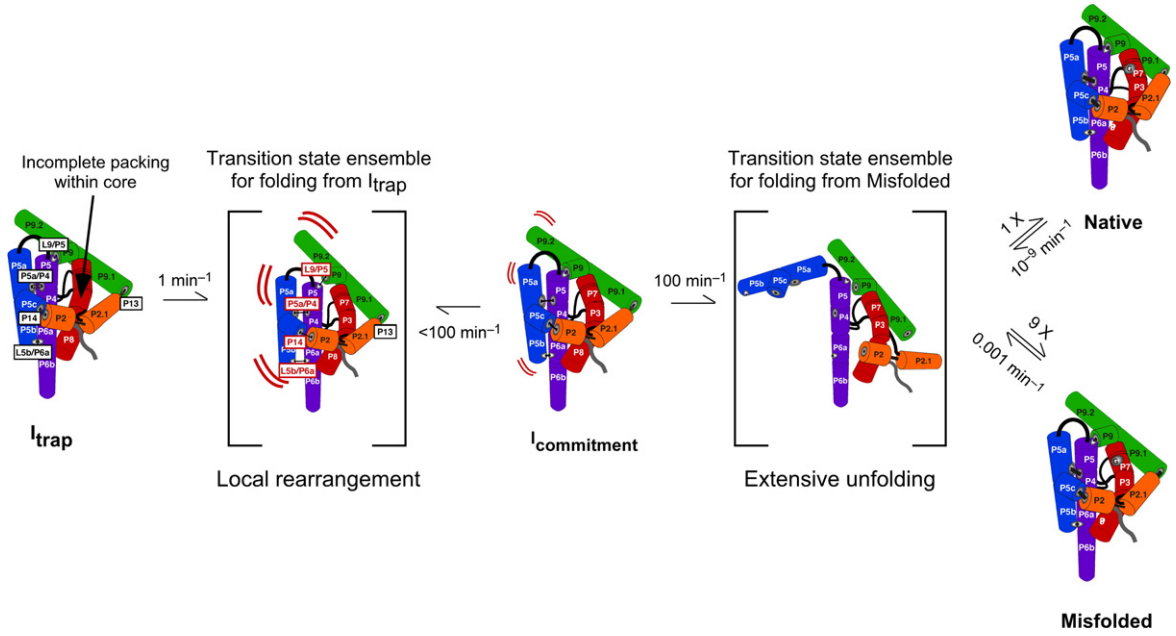

Fig. 5. Model for continued folding of the intermediates I_{trap} and M. The five long-range tertiary contacts are labeled in boxes. The four contacts that accelerate folding from I_{trap} when mutated are labeled in red in the transition state adjacent to I_{trap}. P13 apparently remains formed in the transition state from I_{trap} to the subsequent intermediate $I_{commitment}$ (indicated by the black label). $I_{commitment}$ then continues to unfold more globally and partitions predominantly to M, which then slowly re-folds to N. Folding transitions between $I_{commitment}$, M, and N likely proceed through a large collection of intermediates and transition states that are unfolded to varying degrees and may or may not be the same for the different transitions. For simplicity, the entire collection is shown as a single transition state. The rate constant of 100 min^{-1} from $I_{commitment}$ to this transition state was determined previously by measuring folding starting from conditions that allow avoidance of I_{trap} but not $I_{commitment}$.[21] M then slowly unfolds back to this transition state with a rate constant of 0.001 min^{-1}, giving an observed rate constant of 10^{-4} min^{-1} after accounting for the 10-fold greater likelihood of returning to M rather than proceeding to N. Once reached, the native ribozyme unfolds back to this transition state very slowly. The indicated rate constant of 10^{-9} min^{-1} is calculated from the measured value of 10^5 for the equilibrium between N and M.[35] All of the rate constants shown are from experiments at 25 °C and 10 mM Mg^{2+}.

These measurements also gave insight into the 'decision' in folding between pathways to the native and misfolded conformations, which was shown previously to be made during the transition from I_{trap}.[15] The mutations had at most small effects on the partitioning between folding to the native and misfolded structures (<2-fold, Table S1), consistent with earlier results under similar conditions.[10] The distinct and larger effects of mutations on the folding rate than the choice between pathways suggest that escape from I_{trap} and the commitment to alternative pathways are separate events within the folding process (see Fig. 5). Further support for this model comes from the prior observation of an alternative folding pathway that avoids I_{trap} but gives the same partitioning between the N and M states.[21]

Overall, the large, nearly uniform effects of tertiary contact mutations on re-folding from M, as well as the large *m* value and temperature, Mg^{2+}, and solvent isotope dependences[10] suggest a transition state in which all or nearly all of the tertiary contacts are disrupted and the RNA is globally unfolded. In stark contrast, these dependences are much weaker for I_{trap} and are not uniform. Strikingly, mutation of one of the tertiary elements, P13, gave essentially no effect, despite strong evidence for the presence of P13 in I_{trap} (Fig. 2) and even in the absence of Mg^{2+} under some conditions (Ref. 21; S. Solomatin and D.H., unpublished results). Further, the small *m* value suggests that not all of the peripheral tertiary interactions need be broken to escape from I_{trap}. We therefore suggest a model in which folding from I_{trap} occurs with a *local* disruption of structure, whereas folding from M involves *global* unfolding.

Further development of the model for escape from I_{trap} via local unfolding

The differential effects of peripheral mutations allow us to hone our model for the local unfolding that allows the RNA to escape from the folding intermediate I_{trap} (Fig. 5). Mutations in the region of the molecule within and nearby helices P4 through P6 result in an increased folding rate, whereas mutations that disrupt the P13 tertiary contact, between the loops adjoining P2.1 and P9.1, do not. P13 sits away from the other tertiary contacts in the native molecule, and the considerable compaction of the ribozyme in I_{trap}[16,36] and the evidence for formation of each of the long-range tertiary contacts (Ref. 9 and data herein) suggest that the positioning of these elements within I_{trap} is similar to that in the

native state. Thus, the results suggest that the unfolding to escape from I_{trap} occurs primarily on the P4–P6 side of the molecule (the left side of the RNA in the cartoon shown in Fig. 5). Additional unfolding of other regions may occur after the rate-limiting transition state, as shown in Fig. 5, but would not be detected because it would not influence the overall rate of the transition.

Comparison to prior results provides additional evidence for local unfolding and suggests that the unfolding event on the P4–P6 face is modest, not involving full unraveling of even local structured elements. Folding of the P4–P6 domain involves the close packing of the P5abc subdomain against the helical stack that includes P4, P5, and P6, and folding can readily occur independently of the rest of the molecule.[37,38] The folded structure is stabilized by two tertiary contacts between P5abc and the adjacent helical stack (indicated by arrows in Fig. 1).

There is strong evidence that P4–P6 forms early in folding, prior to formation of I_{trap},[12,27,32,33,39,40] and the two tertiary contacts within P4–P6 have been shown to form stably and with a high degree of cooperativity within the isolated P4–P6 domain (K=12 at 22 °C with 10 mM Mg^{2+} and 200 mM Na^{+} and K=100 under these conditions with 70 mM Mg^{2+}; Ref. 41 and B. Sattin and D.H., unpublished results). Assuming that these contacts are at least as stable in I_{trap}, if escape from I_{trap} required disruption of the contacts, then mutation of either contact would give an acceleration equivalent to its equilibrium constant for formation. In contrast, the effects are modest (5-fold) relative to their equilibrium constants, and the difference between the expected and observed effects is expected to be still larger with increased Mg^{2+} concentration, which increases the stability of the contacts in P4–P6 but does not slow folding from I_{trap}.[15] Thus, the results most simply suggest that disruption of the tertiary contacts facilitates escape from I_{trap} but is not a required event in the unfolding pathway. Presumably, the breaking of peripheral contacts provides more room for moving and reshaping nucleotides within the core, many of which have yet to make their native interactions, and/or weakens fortuitous nonnative interactions within the core that must be broken to allow formation of the native interactions.

Further, the finding that multiple interactions can accelerate unfolding of I_{trap} when they are disrupted, yet their disruptions are not absolutely required for unfolding of I_{trap}, suggests that there are many different pathways for escape from this intermediate. Given the large number of interactions within the ribozyme core and the significant conformational freedom of the single-stranded RNA backbone, the existence of multiple pathways would not be surprising, and there is increasing evidence for such complexities in RNA folding landscapes.[21,32,34,42–44] Understanding more about this complexity and about the structures, dynamics, and energetics that underlie the folding pathways and intermediates remains an important challenge in studies of RNA folding and function.

Native-state formation via successive folding and unfolding steps

After escaping from I_{trap}, a small fraction of the ribozyme folds to the native state, but most progresses to a second kinetically trapped intermediate, M (Fig. 5). For most of the ribozyme, multiple additional cycles of unfolding and re-folding are necessary to achieve native-state formation. The intermediate M is similar in structure to the native state overall, as revealed by structure and functional probing, but is very slow to convert to N. Escape from M requires large-scale unfolding of the molecule, most likely to unravel a topological isomer with an incorrect strand crossing within the ribozyme's core.[10]

The intermediate M also bears a strong resemblance to I_{trap}, and it is interesting to consider why the properties of their folding transitions are so different. Although the peripheral tertiary interactions appear to be formed (Ref. 9 and data herein) and the elements that comprise these interactions are likely in their native or near-native positions in the I_{trap} intermediate, as noted above, the central catalytic core is not protected from solvent in I_{trap} and is presumably not formed or not correctly formed. Conversion of I_{trap} to M or N involves protections of the central core from solvent-based probes, suggesting increased packing in the molecule's center.

Formation of the peripheral contacts gives only small and variable slowing of the rearrangement of I_{trap}, but these contacts strongly and nearly uniformly inhibit the escape from M.[10] The large effects of mutation of any of the long-range contacts on folding from M most simply suggest that all of the contacts are disrupted during the transition to N, as shown in Fig. 5. To account for the much larger effects on M than I_{trap}, we suggest a model in which the peripheral contacts are strengthened as folding progresses from I_{trap} to M, likely arising at least in part from increased cooperativity. Supporting a model of long-range cooperativity, one of the peripheral elements, P5abc, was shown to stabilize the native state relative to M, by 6 kcal mol^{-1}, by generating greater cooperativity with tertiary contacts away from P4–P6 (Ref. 35; T. Johnson and R.R., unpublished results). Other peripheral elements have been shown to be important in stabilizing the native state in its active conformation (Ref. 45; T. Benz-Moy and D.H., unpublished results). Although it remains to be demonstrated experimentally, the presence of a portion of this cooperativity in the M state would provide a simple explanation for the large and nearly uniform effects of mutations, as ablation of any contact in the network would also weaken the other contacts.

Together, these and prior results suggest an intriguing progression of increased cooperativity within the RNA as folding progresses. Indeed, the formation of interconnected, cooperative structures may present a challenge to RNA folding, requiring RNAs to undergo multiple rounds of folding and

unfolding as they traverse complex and rugged energy landscapes. Initial and simultaneous formation of a full network of native interactions would presumably be unlikely for all but the simplest RNAs, especially given the considerable freedom of motion of the RNA backbone and its propensity to form alternative structures. Local unfolding and rearrangement may then allow new native contacts to form and energetic connectivity to increase. If there are no large-scale errors in folding, such processes may lead to formation of the native state. However, if large-scale unfolding is necessary to resolve non-native regions, as observed here, the same local rearrangements would be expected to increase the difficulty of subsequent folding steps that involve extensive unfolding, leading to progressively larger energy barriers through the folding process.

Materials and Methods

Materials

The L-21/ScaI *Tetrahymena* ribozyme was purified using Qiagen RNeasy columns as previously described.[46] trations of wild-type and variant ribozymes were determined spectrophotometrically using an extinction coefficient of 3.9×10^6 M^{-1} cm^{-1}. The oligonucleotide substrate was synthesized using standard solid-phase methods by the Protein and Nucleic Acid Facility at Stanford, 5′-end-labeled with [γ-^{32}P]ATP using T4 polynucleotide kinase, and purified by non-denaturing polyacrylamide gel electrophoresis as previously described.[47]

Hydroxyl radical footprinting

Hydroxyl radical footprinting was performed using 'Fast Fenton Footprinting' conditions.[22] Folding of 5′- or 3′-^{32}P-labeled ribozyme was initiated at 25 °C by adding 10 mM Mg^{2+} in 50 mM Na–Mops, pH 7.0, and 0.2% H_2O_2 and allowed to proceed for 15 or 30 s to generate a population of predominantly I_{trap}.[11,15] The footprinting patterns from these two incubation times were the same within error, and both sets of data were included in the reported values for I_{trap}. Footprinting was then initiated by adding Fenton reagents [5 mM $(NH_4)_2Fe(II)(SO_4)_2$ and 6.25 mM ethylene dinitrilotetraacetic acid, with Na–Mops and Mg^{2+} concentrations maintained at 50 and 10 mM, respectively, and H_2O_2 diluted to a final concentration of 0.15%]. After 30 s of footprinting, reactions (12 μl) were quenched by addition of 2 vol of ethanol (25 μl) and 1/10 vol of 3 M Na-acetate (1.2 μl). RNA was pelleted by centrifugation, and cleavage products were separated by 8% denaturing PAGE, imaged using a Phosphorimager (Amersham Biosciences, Piscataway, NJ), and quantified using the single-band fitting program SAFA.[48] Intensity values were normalized relative to the average intensity from the range of nucleotides quantitated for each lane, and normalized values from three to four independent determinations were averaged (with the exception of nucleotides 30–40, which were only probed once). For each secondary-structure depiction of Fig. 2 and Fig. S1, the average normalized values for each nucleotide from one ribozyme conformer were subtracted from those of another conformer to obtain difference values, which are displayed on a color scale as indicated. In Fig. 2d and e, nucleotide segments are highlighted in blue or yellow if at least two consecutive nucleotides had differences of at least 0.2 in their average values. From this two-nucleotide 'nucleus', the boundaries of the segment to be colored were established walking outward in each direction until either of the following were reached: (1) two consecutive nucleotides with difference values of less than 0.1 or (2) a nucleotide with a difference value of less than 0, that is, where the protection or enhancement was reversed.

DMS footprinting

DMS footprinting was performed essentially as previously described.[10,24,26] Reactions contained 2 μM L-21/ScaI ribozyme in 25 μl of 50 mM Na–Mops, pH 7.0, and 10 mM Mg^{2+} solution at 15 °C. To give maximal population of I_{trap} for footprinting, we folded the ribozyme at 15 °C in the presence of Mg^{2+} for 1 min, followed by addition of DMS (1 μl of 16% DMS in ethanol) to a final concentration of 0.64%. DMS was allowed to react with the ribozyme for 1 min. The previously determined rate constant of 0.15 min^{-1} for decay of I_{trap} to M and N at 15 °C indicates that 85% of the population remains in the I_{trap} form at the time of DMS addition and 75% remains at the end of DMS treatment (Ref. 20, see Scheme 1c). DMS reactions were quenched and processed as previously described[10] and analyzed using SAFA.[48] Band intensity values were normalized by dividing by the intensity of the fully extended product, and results from two to four independent determinations were averaged. The final intensity values were multiplied by an arbitrary scaling factor of 800 to allow comparison with hydroxyl radical results on the same scale, as shown in Fig. 2 and Fig. S1. In these figures, asterisks denote the most prominent changes in DMS footprinting, as defined by a change in the intensity values of at least 0.2 and a relative change of at least 30%. This analysis avoids nucleotides that are modified by DMS so strongly that they change in reactivity from one ribozyme form to another by a large amount and are therefore colored strongly, but whose changes are small relative to their total signal and therefore are likely to be less significant.

Catalytic activity measurements to follow formation of the native state

Folding transitions from the I_{trap} and M intermediates to the native state were followed by the onset of enzymatic activity as described previously.[15,20,30] Briefly, folding from I_{trap} was followed by initiating Mg^{2+}-induced folding in the presence of a trace amount of radiolabeled oligonucleotide substrate (S) and saturating concentration of guanosine under the desired solution conditions (50 mM Na–Mops, pH 7.0, 50 mM Mg^{2+} at 25 °C or 50 mM Na–Mops, pH 7.0, 50 mM Mg^{2+} at 11 °C). Progress curves displayed a burst of product formation, which is rate-limited by the folding transition from I_{trap} to N and M, followed by a slower product formation that is rate-limited by release of substrate from the misfolded ribozyme and re-binding by the native ribozyme. Control experiments (Ref. 10 and data not shown) established that under the conditions used to follow folding, each ribozyme mutant gives a rate constant for S cleavage that is large enough to ensure that folding remains rate-limiting in experiments designed to measure folding.

Re-folding from M was followed by first incubating with 10 mM Mg^{2+} for 10–20 min at 25 °C (50 mM Na–Mops, pH 7.0) to form M (90% of the ribozyme population), then transferring the reaction to 50 mM Mg^{2+} at 25 °C. At various times, aliquots were removed and the fraction of native ribozyme was determined from the fraction of input substrate that was cleaved in a rapid burst, as described previously.[10,15,30]

Acknowledgements

This work was funded by National Institutes of Health Grant R01-GM49243 (to D.H.), National Institutes of Health Grant R01-GM070456 (to R.R.), and Welch Foundation Grant F-1563 (to R.R.).

Supplementary Data

Supplementary data associated with this article can be found, in the online version, at doi:10.1016/j.jmb.2010.06.010

References

1. Treiber, D. K. & Williamson, J. R. (1999). Exposing the kinetic traps in RNA folding. *Curr. Opin. Struct. Biol.* **9**, 339–345.
2. Thirumalai, D. & Woodson, S. A. (2000). Maximizing RNA folding rates: a balancing act. *RNA*, **6**, 790–794.
3. Russell, R. (2008). RNA misfolding and the action of chaperones. *Front. Biosci.* **13**, 1–20.
4. Schroeder, R., Barta, A. & Semrad, K. (2004). Strategies for RNA folding and assembly. *Nat. Rev., Mol. Cell Biol.* **5**, 908–919.
5. Woodson, S. A. (2008). RNA folding and ribosome assembly. *Curr. Opin. Chem. Biol.* **12**, 667–673.
6. Sykes, M. T. & Williamson, J. R. (2009). A complex assembly landscape for the 30S ribosomal subunit. *Annu. Rev. Biophys.* **38**, 197–215.
7. Pan, J., Thirumalai, D. & Woodson, S. A. (1997). Folding of RNA involves parallel pathways. *J. Mol. Biol.* **273**, 7–13.
8. Pan, T. & Sosnick, T. R. (1997). Intermediates and kinetic traps in the folding of a large ribozyme revealed by circular dichroism and UV absorbance spectroscopies and catalytic activity. *Nat. Struct. Biol.* **4**, 931–938.
9. Treiber, D. K., Rook, M. S., Zarrinkar, P. P. & Williamson, J. R. (1998). Kinetic intermediates trapped by native interactions in RNA folding. *Science*, **279**, 1943–1946.
10. Russell, R., Das, R., Suh, H., Travers, K. J., Laederach, A., Engelhardt, M. A. & Herschlag, D. (2006). The paradoxical behavior of a highly structured misfolded intermediate in RNA folding. *J. Mol. Biol.* **363**, 531–544.
11. Russell, R., Tijerina, P., Chadee, A. B. & Bhaskaran, H. (2007). Deletion of the P5abc peripheral element accelerates early and late folding steps of the *Tetrahymena* group I ribozyme. *Biochemistry*, **46**, 4951–4961.
12. Zarrinkar, P. P. & Williamson, J. R. (1994). Kinetic intermediates in RNA folding. *Science*, **265**, 918–924.
13. Emerick, V. L. & Woodson, S. A. (1994). Fingerprinting the folding of a group I precursor RNA. *Proc. Natl Acad. Sci. USA*, **91**, 9675–9679.
14. Downs, W. D. & Cech, T. R. (1996). Kinetic pathway for folding of the *Tetrahymena* ribozyme revealed by three UV-inducible crosslinks. *RNA*, **2**, 718–732.
15. Russell, R. & Herschlag, D. (2001). Probing the folding landscape of the *Tetrahymena* ribozyme: commitment to form the native conformation is late in the folding pathway. *J. Mol. Biol.* **308**, 839–851.
16. Russell, R., Millett, I. S., Doniach, S. & Herschlag, D. (2000). Small angle X-ray scattering reveals a compact intermediate in RNA folding. *Nat. Struct. Biol.* **7**, 367–370.
17. Michel, F. & Westhof, E. (1990). Modelling of the three-dimensional architecture of group I catalytic introns based on comparative sequence analysis. *J. Mol. Biol.* **216**, 585–610.
18. Lehnert, V., Jaeger, L., Michel, F. & Westhof, E. (1996). New loop–loop tertiary interactions in self-splicing introns of subgroup IC and ID: a complete 3D model of the *Tetrahymena thermophila* ribozyme. *Chem. Biol.* **3**, 993–1009.
19. Cannone, J. J., Subramanian, S., Schnare, M. N., Collett, J. R., D'Souza, L. M., Du, Y. *et al.* (2002). The comparative RNA web (CRW) site: an online database of comparative sequence and structure information for ribosomal, intron, and other RNAs. *BMC Bioinformatics*, **3**, 2.
20. Russell, R. & Herschlag, D. (1999). New pathways in folding of the *Tetrahymena* group I RNA enzyme. *J. Mol. Biol.* **291**, 1155–1167.
21. Russell, R., Zhuang, X., Babcock, H. P., Millett, I. S., Doniach, S., Chu, S. & Herschlag, D. (2002). Exploring the folding landscape of a structured RNA. *Proc. Natl Acad. Sci. USA*, **99**, 155–160.
22. Shcherbakova, I., Mitra, S., Beer, R. H. & Brenowitz, M. (2006). Fast Fenton footprinting: a laboratory-based method for the time-resolved analysis of DNA, RNA and proteins. *Nucleic Acids Res.* **34**, e48.
23. Qu, H. L., Michot, B. & Bachellerie, J. P. (1983). Improved methods for structure probing in large RNAs: a rapid 'heterologous' sequencing approach is coupled to the direct mapping of nuclease accessible sites. Application to the 5′ terminal domain of eukaryotic 28S rRNA. *Nucleic Acids Res.* **11**, 5903–5920.
24. Inoue, T. & Cech, T. R. (1985). Secondary structure of the circular form of the *Tetrahymena* rRNA intervening sequence: a technique for RNA structure analysis using chemical probes and reverse transcriptase. *Proc. Natl Acad. Sci. USA*, **82**, 648–652.
25. Moazed, D., Stern, S. & Noller, H. F. (1986). Rapid chemical probing of conformation in 16 S ribosomal RNA and 30 S ribosomal subunits using primer extension. *J. Mol. Biol.* **187**, 399–416.
26. Tijerina, P., Mohr, S. & Russell, R. (2007). DMS footprinting of structured RNAs and RNA-protein complexes. *Nat. Protoc.* **2**, 2608–2623.
27. Sclavi, B., Sullivan, M., Chance, M. R., Brenowitz, M. & Woodson, S. A. (1998). RNA folding at millisecond intervals by synchrotron hydroxyl radical footprinting. *Science*, **279**, 1940–1943.
28. Pan, J. & Woodson, S. A. (1998). Folding intermediates of a self-splicing RNA: mispairing of the catalytic core. *J. Mol. Biol.* **280**, 597–609.
29. Treiber, D. K. & Williamson, J. R. (2001). Concerted kinetic folding of a multidomain ribozyme with a disrupted loop–receptor interaction. *J. Mol. Biol.* **305**, 11–21.

30. Wan, Y., Mitchell, D. & Russell, R. (2010). Catalytic activity as a probe of native RNA folding. *Methods Enzymol.* **468**, 195–218.
31. Shelton, V. M., Sosnick, T. R. & Pan, T. (1999). Applicability of urea in the thermodynamic analysis of secondary and tertiary RNA folding. *Biochemistry*, **38**, 16831–16839.
32. Laederach, A., Shcherbakova, I., Liang, M. P., Brenowitz, M. & Altman, R. B. (2006). Local kinetic measures of macromolecular structure reveal partitioning among multiple parallel pathways from the earliest steps in the folding of a large RNA molecule. *J. Mol. Biol.* **358**, 1179–1190.
33. Shcherbakova, I. & Brenowitz, M. (2005). Perturbation of the hierarchical folding of a large RNA by the destabilization of its scaffold's tertiary structure. *J. Mol. Biol.* **354**, 483–496.
34. Laederach, A., Shcherbakova, I., Jonikas, M. A., Altman, R. B. & Brenowitz, M. (2007). Distinct contribution of electrostatics, initial conformational ensemble, and macromolecular stability in RNA folding. *Proc. Natl Acad. Sci. USA*, **104**, 7045–7050.
35. Johnson, T. H., Tijerina, P., Chadee, A. B., Herschlag, D. & Russell, R. (2005). Structural specificity conferred by a group I RNA peripheral element. *Proc. Natl Acad. Sci. USA*, **102**, 10176–10181.
36. Russell, R., Millett, I. S., Tate, M. W., Kwok, L. W., Nakatani, B., Gruner, S. M. *et al.* (2002). Rapid compaction during RNA folding. *Proc. Natl Acad. Sci. USA*, **99**, 4266–4271.
37. Murphy, F. L. & Cech, T. R. (1993). An independently folding domain of RNA tertiary structure within the *Tetrahymena* ribozyme. *Biochemistry*, **32**, 5291–5300.
38. Cate, J. H., Gooding, A. R., Podell, E., Zhou, K., Golden, B. L., Kundrot, C. E. *et al.* (1996). Crystal structure of a group I ribozyme domain: principles of RNA packing. *Science*, **273**, 1678–1685.
39. Kwok, L. W., Shcherbakova, I., Lamb, J. S., Park, H. Y., Andresen, K., Smith, H. *et al.* (2006). Concordant exploration of the kinetics of RNA folding from global and local perspectives. *J. Mol. Biol.* **355**, 282–293.
40. Schlatterer, J. C., Kwok, L. W., Lamb, J. S., Park, H. Y., Andresen, K., Brenowitz, M. & Pollack, L. (2008). Hinge stiffness is a barrier to RNA folding. *J. Mol. Biol.* **379**, 859–870.
41. Sattin, B. D., Zhao, W., Travers, K., Chu, S. & Herschlag, D. (2008). Direct measurement of tertiary contact cooperativity in RNA folding. *J. Am. Chem. Soc.* **130**, 6085–6087.
42. Pan, T., Fang, X. & Sosnick, T. (1999). Pathway modulation, circular permutation and rapid RNA folding under kinetic control. *J. Mol. Biol.* **286**, 721–731.
43. Ditzler, M. A., Rueda, D., Mo, J., Hakansson, K. & Walter, N. G. (2008). A rugged free energy landscape separates multiple functional RNA folds throughout denaturation. *Nucleic Acids Res.* **36**, 7088–7099.
44. Solomatin, S. V., Greenfeld, M., Chu, S. & Herschlag, D. (2010). Multiple native states reveal persistent ruggedness of an RNA folding landscape. *Nature*, **463**, 681–684.
45. Engelhardt, M. A., Doherty, E. A., Knitt, D. S., Doudna, J. A. & Herschlag, D. (2000). The P5abc peripheral element facilitates preorganization of the *Tetrahymena* group I ribozyme for catalysis. *Biochemistry*, **39**, 2639–2651.
46. Russell, R. & Herschlag, D. (1999). Specificity from steric restrictions in the guanosine binding pocket of a group I ribozyme. *RNA*, **5**, 158–166.
47. Zaug, A. J., Grosshans, C. A. & Cech, T. R. (1988). Sequence-specific endoribonuclease activity of the *Tetrahymena* ribozyme: enhanced cleavage of certain oligonucleotide substrates that form mismatched ribozyme-substrate complexes. *Biochemistry*, **27**, 8924–8931.
48. Das, R., Laederach, A., Pearlman, S. M., Herschlag, D. & Altman, R. B. (2005). SAFA: semi-automated footprinting analysis software for high-throughput quantification of nucleic acid footprinting experiments. *RNA*, **11**, 344–354.